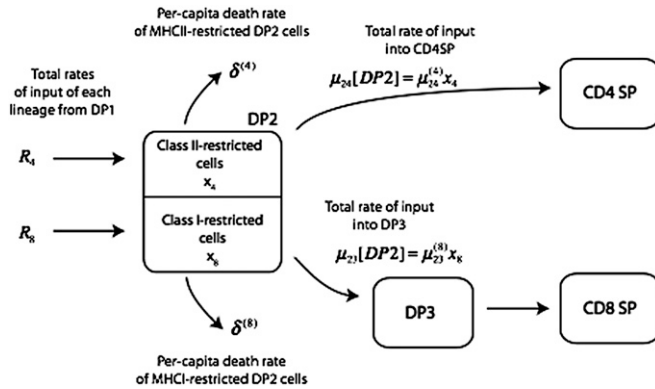


Supporting Information

Sinclair et al. 10.1073/pnas.1304859110

SI Methods

Recall that in the controls, the overall dynamics of the double-positive (DP) 2 stage of development are described by



$$\frac{d[DP2]}{dt} = \mu_{12}[DP1] - (\delta_2 + \mu_{23} + \mu_{24})[DP2].$$

However, DP2 comprises class II- and class I-restricted populations whose numbers are x_4 and x_8 , respectively. Let the total rate of flow of the two lineages into DP2 at steady state in the controls be R_4 and R_8 , which are unknown. The dynamics of the two lineages in DP2 are then modeled as (refer to the graphic shown above)

$$\frac{dx_4}{dt} = R_4 - (\mu_{24}^{(4)} + \delta^{(4)})x_4$$

$$\frac{dx_8}{dt} = R_8 - (\mu_{23}^{(8)} + \delta^{(8)})x_8,$$

where the superscripts refer to lineage-specific per-cell rates and the subscripts on maturation rates follow the same convention as the parameters in the main model. Note we assume that class II-restricted cells are not misdirected into DP3 in the controls (because the DP3 death rate is low in controls, as discussed in the main text).

At steady state, the equations above give R_4/R_8 directly as a function of the (unknown) parameters $\mu_{24}^{(4)}$, $\mu_{23}^{(8)}$, $\delta^{(4)}$, $\delta^{(8)}$, x_4 , and x_8 :

$$\frac{R_4}{R_8} = \frac{\mu_{24}^{(4)} + \delta^{(4)} x_4}{\mu_{23}^{(8)} + \delta^{(8)} x_8}. \quad [S1]$$

We can eliminate three of these parameters using the following information:

i) Total rate of DP2 into CD4 SP (% thymus per day): $x_4 \mu_{24}^{(4)} = \mu_{24}[DP2]$

ii) Total rate of DP2 into DP3 (% thymus per day): $x_8 \mu_{23}^{(8)} = \mu_{23}[DP2]$

iii) Total rate of cell loss in DP2 (% thymus per day): $x_4 \delta^{(4)} + x_8 \delta^{(8)} = \delta_2[DP2]$

iv) DP2 compartment size: $[DP2] = x_4 + x_8$

The rate constants on the right-hand side of constraints *i-iii* are the measured DP2-wide rate constants estimated for the control group. [These are all the constraints available. The estimated flux rate into DP2, $\mu_{12}[DP1]$, provides no additional information because it equals the sum of the three DP2 exit rates (*i-iii*) at equilibrium. Similarly, the estimates of the exit rates from CD4 SP and DP3 do not add information; these must necessarily be equal to DP2 exit rates *i* and *ii*, respectively.]

The steady-state compartment size $[DP2]$ disappears from the calculation, and these constraints reduce Eq. S1 to two simultaneous equations in three unknowns:

$$\frac{R_4}{R_8} = \frac{\mu_{24} + f \delta^{(4)}}{\mu_{23} + (1-f) \delta^{(8)}} \quad [S2]$$

$$\delta_2 = f \delta^{(4)} + (1-f) \delta^{(8)},$$

where f is the proportion of DP2 that is class II-restricted, $x_4/(x_4 + x_8)$. We can eliminate one of the three parameters here; we choose to eliminate f , and obtain

$$\frac{R_4}{R_8} = \frac{\mu_{24}(\delta^{(8)} - \delta^{(4)}) + \delta^{(4)}(\delta^{(8)} - \delta_2)}{\mu_{23}(\delta^{(8)} - \delta^{(4)}) - \delta^{(8)}(\delta^{(4)} - \delta_2)} \equiv g(\delta^{(4)}, \delta^{(8)}), \quad [S3]$$

which is a function of two unknowns: the death rates of class I- and class II-restricted cells in DP2, $\delta^{(8)}$ and $\delta^{(4)}$.

Eq. S2 then allows us to solve for f directly, using the known DP2-wide death rate $\delta_2 = f \delta^{(4)} + (1-f) \delta^{(8)} = 0.50$. Using the point estimates for $\delta^{(8)}$ and $\delta^{(4)}$ (main text) yields $f = 0.64$, meaning that 64% of cells at the DP2 stage are class II-restricted at equilibrium. This information allows us to estimate the maturation rates $\mu_{24}^{(4)}$ and $\mu_{23}^{(8)}$, because these must be their compartment-averaged counterparts divided by the frequency at which each population is present. At the point estimates,

$$\mu_{24}^{(4)} = \mu_{24}/f = 0.139/0.64 = 0.22$$

$$\mu_{23}^{(8)} = \mu_{23}/(1-f) = 0.073/(1-0.64) = 0.20.$$

Thus, with these death rates in DP2, we find that the enrichment of the CD4 lineage in DP2 comes predominantly from differential death in DP2 and not from asymmetry in precursors arriving from DP1 or different rates of maturation out of DP2.

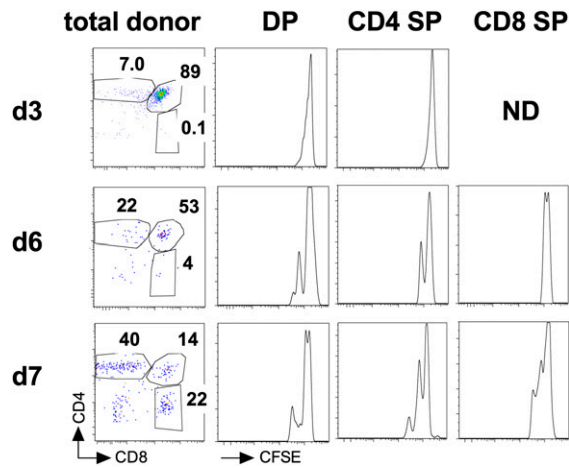


Fig. S1. Limited cell division by thymocytes undergoing selection. DP1 thymocytes from CD45.1 donor mice were purified by cell sorting, labeled with carboxyfluorescein succinimidyl ester (CFSE) cell dye, and injected intrathymically into CD45.2 hosts. At days 3, 6, and 7 after transfer, groups of mice ($n = 2$) were killed and CD45.1⁺ donor cells were analyzed by flow cytometry. Dot plots are of CD4 vs. CD8 expression by CD45.1⁺CD45.2⁻-gated cells. Histograms are of CFSE label by total DP, CD4 SP, and CD8 SP thymocyte populations. N.D., not detectable.

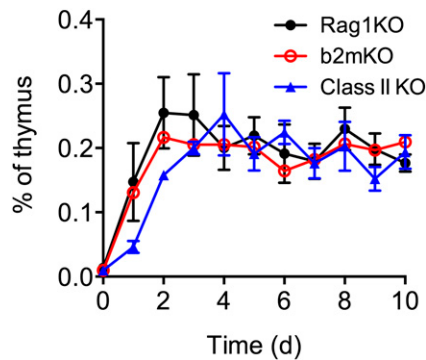


Fig. S2. Intraepithelial precursor development is similar in $b2m^{-/-}$ and $Mhc-II^{-/-}$ tetracycline-inducible Zap70 transgene (TetZap70) chimeras. Irradiation chimeras were generated using bone marrow from TetZap70 donors to reconstitute $Rag1^{-/-}$, $b2m^{-/-}Rag1^{-/-}$, and $Mhc-II^{-/-}Rag1^{-/-}$ hosts. Six weeks later, mice were fed doxycycline to induce Zap70 expression. Groups of mice were taken at days 0–10, and frequencies of intraepithelial precursor cells [CD4^{lo} CD8 double-negative CD44^{lo} heat-stable antigen (hSA)^{hi}CD5^{hi} T-cell receptor (TCR)^{int}] were determined by fluorescence-activated cell sorting ($n > 8$ per day). Graphs show the percentage of total thymocytes \pm SD in $Rag1^{-/-}$ (black), $b2m^{-/-}Rag1^{-/-}$ (red), and $Mhc-II^{-/-}Rag1^{-/-}$ (blue) KO hosts. Data are pooled from three or more independent experiments.

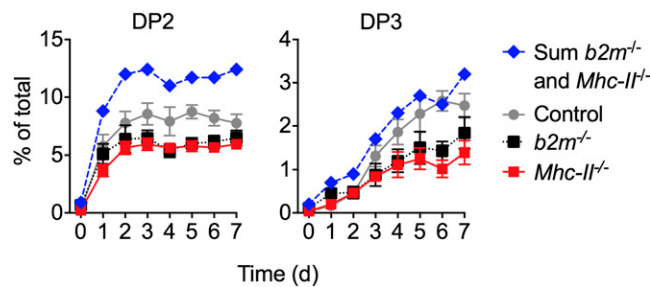


Fig. S3. Separate development of class I- and class II-restricted DP2 thymocytes is not additive when they develop in the same host. Graphs are of the percentage of total thymus of the indicated subset in time courses of TetZap70 thymocyte development from Fig. 2. In addition, mixed color symbols depict the sum of frequencies from $b2m^{-/-}$ and $Mhc-II^{-/-}$ host time courses. Data are pooled from two or more experiments for each subset tested.